

# Inertial-Electrostatic-Fusion Propulsion Spectrum: Air-Breathing to Interstellar Flight

by Robert W. Bussard and Lorin W. Jameson, Energy/Matter Conversion Corporation, 680 Garcia Street, Santa Fe, NM 87505, <[emc2qed@comcast.net](mailto:emc2qed@comcast.net)>

## Abstract

A new inertial-electrostatic-fusion direct electric power source can be used to drive a relativistic e-beam (REB) to heat propellant. The resulting system is shown to yield specific impulse and thrust/mass ratio 2-3 orders of magnitude larger than from other advanced propulsion concepts. This quiet-electric-discharge system can be applied to aerospace vehicles from air-breathing to near-interstellar flight. Examples are given for Earth/Mars flight missions that show transit times of 40 days with 20% payload in single-stage vehicles.

$P_e, P_{net}$	= electric power, MW <sub>e</sub>
$P_f$	= fusion power, MW <sub>tb</sub>
$P_L$	= propulsive jet thrust power
$P_o$	= normalized power
$t_b$	= engine thrusting time
$t_c$	= vehicle coasting time
$v$	= vehicle speed
$\delta S$	= incremental distance traversed
$\delta v_c$	= characteristic velocity of flight

## Nomenclature

$A_{rad}$	= waste heat radiator area
$a_f$	= final vehicle force acceleration
$a_{rad}$	= radiator mass coefficient
$a_o$	= initial vehicle force acceleration
$F$	= thrust
$F_o$	= normalized thrust
$[F]$	= engine system thrust/mass ratio
$G_{gross}$	= ratio gross electric to drive power
$I_s$	= net effective $I_{sp}$
$I_{sp}$	= engine system specific impulse
$I_o$	= normalized $I_{sp}$
$K_{iex}$	= magnet mass factor for EXL QED
$m_{-e}, M_L$	= engine system mass
$m_{-l}, M_l$	= payload mass
$m_{-p}$	= propellant mass
$m_{-o}, M_o$	= vehicle gross mass

## 1. Introduction

The achievement of effective space flight requires propulsion systems of large flight-path-averaged specific impulse  $I_{sp}$ , and engine system thrust-to-mass ratio  $F/m_{-e} = [F]$ .

If  $[F]$  is greater than the local gravitational acceleration, then all flights will be "high-thrust" in character, and minimal transit times can be achieved for any vehicle configuration and mass distribution. With such engines, economically useful payload fractions can be carried over large-velocity increments by single-stage vehicles with practical structural factors. For short transit times in most missions it is found that the limited energy available from chemical combustion reactions limits payload fractions to small values, even with multiple-stage vehicles, and single-stage vehicles are not feasible for rapid (e.g., less than 1 year) interplanetary flights. Greater payload fractions with short flight time can be achieved only with high  $I_{sp}$ , engines<sup>1</sup> that also have high-thrust capabilities.

But this can be achieved only if a sufficiently energetic propulsion system can be found to drive these vehicles. Nuclear sources far exceed the specific energy limits<sup>2</sup> of chemical combustion, but the inherent high  $I_{sp}$  advan-

tages of most nuclear fission propulsion concepts are compromised by inherent hazardous radiation output. The resulting massive shielding requirements negate most of the performance improvements derived from such high-energy sources.<sup>4</sup>

Yet energetic nuclear reactions exist that do not yield radiation requiring such shielding. These are fusion reactions between ions of certain isotopes of the lighter elements; specifically H(p) and <sup>11</sup>B, <sup>6</sup>Li/<sup>7</sup>Li and <sup>9</sup>Be, and between <sup>3</sup>He alone and with D (second isotope of hydrogen). Nuclear fusion reactions between these isotopes yield only energetic charged particles (no neutrons) that can be contained with electric and magnetic fields. Also, because the reaction products are charged particles, it is possible (based on past work<sup>6,7</sup> at Department of Energy labs), to convert their energy efficiently directly to electricity.

With these clean reactions, radiation-free fusion-electric powerplants can be made using new methods for dynamic confinement of fusion-reactive ions by special magnetic-electric-potential means,<sup>8</sup> or by inertial-collisional-compression (ICC)<sup>9</sup> of plasma fuel ions. Figures 1 and 2 show the basic principles of these inertial-electrostatic-fusion (IEF) sources.

Both systems accelerate ions radially to a central convergence point (core) by electrical fields in a quasi-spherical geometry. The first of these uses radial electric fields supplied across concentric spherical grids to accelerate ions to the core; this is called the IXL system. The second accelerates the ions by the electric field gradient in a negative potential well maintained by injection of energetic electrons into a confining polyhedral magnetic field configuration; this is the EXL system. Ions converge to a very high density at the system center, and there react and yield energetic, charged fusion products.

Electric power can be obtained from direct conversion of these radially moving fusion product ions escaping the active region by surrounding the electric confinement volume with an electrically biased grid system that decelerates these ions. The resulting power appears in the external conductors of the system, and can be used to drive a unique e-beam-driven, electrically powered rocket engine system of extremely high performance. Concept design studies<sup>10</sup> suggest that such charged-particle quiet-electric-discharge (QED) engines might yield:

1. Air-breathing engines of zero fuel consumption with  $6 < [F] < 12$  and  $2000 < I_{sp} < 4000$  s ( $\{I_{sp} | [F]\} = 24,000$  s), or
2. Rocket propulsion thrust systems with performance parameters varying as  $[F] = 1E4/I_{sp}$ , 0.07, over an  $I_{sp}$ , range from 1500 to 1E5 s.

## IXL - Ion Acceleration

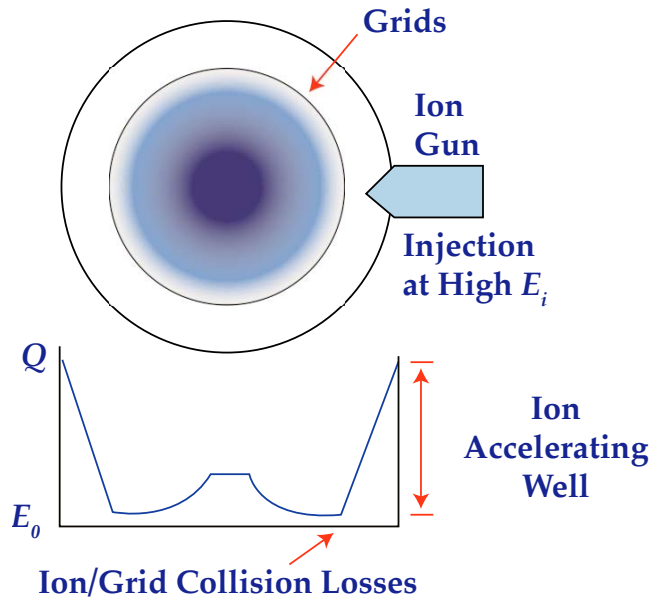


Figure 1 — Ion acceleration in spherical geometry by electrically biased grids; the IXL system

## EXL - Electron Acceleration

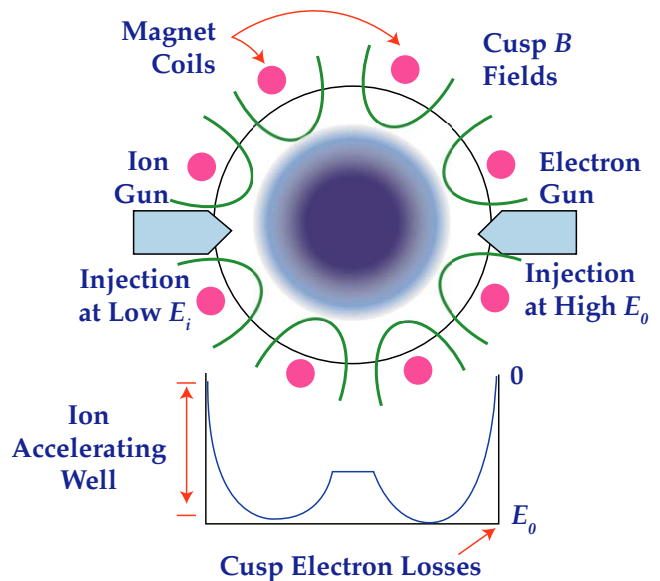


Figure 2 — Ion acceleration in electron-driven negative potential well; the EXL system

## A. Fusion-Electric Rocket Engine Concepts

The achievement of such performance requires efficient direct conversion of energetic charged reaction products from non-radiative fusion systems with large reaction rate densities.

This is readily possible for the fuel combination  $p^{11}B$ , because its products are 3  ${}^4He$  ions at predictable energies of about 2.4 and 3.9 MeV. The small spread in the energy of these particles allows very high direct conversion efficiency to be attained by the decelerating external grid system. This needs to be operated at a maximum voltage of only about 2 MeV, because the  ${}^4He$  ions are all doubly charged ( $Z = 2$ ). The high-voltage electrical power thus produced may be used directly without significant power conditioning (or after some voltage down-conversion) to drive high voltage electron beams at modest currents (ca. a few thousand amps) for direct heating of air or propellant, as well as to power the fusion device itself.

For air-breathing propulsion, the e-beam can be raster-scanned through the underbody flowfield of an external compression hypersonic engine system,<sup>11</sup> thus heating the air to propulsive enthalpy conditions. For rocket propulsion, electron beams at energies of a few MeV or less can deposit their energy directly (and efficiently) into the central regions of a high-pressure gas confined by rotational hydrodynamic flow in a quasi-cylindrical volume. This heating chamber and nozzle constitute the thrust chamber. It is important to note that this means of energy deposition is not that of a conventional low-voltage high-current ohmic-resistive arc (e.g., an arcjet). Since the electron energies are at the lower limit of relativistic electron beam (reb) energies, such e-beam-driven systems are called "reb" heating systems.

Gas heated in this way can be extracted from the chamber core to yield thrust from an expanding flow through an exit nozzle on the heating chamber axis to provide thrust as an e-beam-heated fusion-electric rocket engine. Chamber and nozzle wall insulation by use of axial magnetic fields in such reb-heated devices can reduce gas/wall heat transfer by 1-2 orders of magnitude from conventional convective processes. By these means net effective specific impulse of hydrogen propellant may be  $I_{sp} = 2500-6000$  s (corresponding to temperatures of about 20,000-120,000 K, depending on dissociation/recombination effects, without presenting intractable wall cooling difficulties. Water, ammonia, methane, and other low-molecular-weight fluids can be driven to equally high thrust-chamber core-gas temperatures.

The high-thrust and high performance of QED rocket engines allows large payload fractions to be carried by single-stage aerospace vehicle systems over large incremental velocity changes: payload fractions may be comparable to those of today's conventional high-subsonic commercial aircraft.

Application to space flight is equally beneficial, payload fractions and characteristic velocity increments in cis-lunar and interplanetary missions will all be larger than those from chemical rockets by factors of 3-5, in single-

stage vehicles. Two or more QED stages could be used if very large payloads are desired.

Since all of the propellant heating is done by direct deposition of the reb, the electron flow must close upon the system structure in order to maintain net charge neutrality. Return current conductors must connect the exit nozzle surface with the QED fusion-electric source, and residual back-flowing electron current outside the system will be collected on the vehicle external surface by a collector plate connected to this source, to close the electrical loop.

In space flight, the return current will flow largely through the direct conductors. Residual electrons that leave the nozzle will return through the low-density space plasma surrounding the vehicle. In air-breathing atmospheric flight, using the raster-scanned e-beam direct-air-heating, the large electron current passing through the underbody airflow field will create significant  $O_2$  dissociation and excitation-ionization sites for ozone generation by  $O_2^+$  attachment of dissociated O atoms, to yield copious ozone production by the reaction  $3O_2 + 69.0 \text{ kcal} \rightarrow 2O_3$  (about 48.07 kJ/g of ozone). No further consideration is given here to the direct air-heating system.

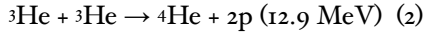
## B. Fusion Electric Power Source

The electric power source for such propulsion engines can be achieved by electrostatic dynamic confinement of the desired charged particle reactions between the special light isotopes of interest. Directions for the research and development toward this goal are well-defined from results of past studies of this problem. These showed the general feasibility of the concept and approach, through the development of comprehensive point models of the fusion device, with technical conceptual design considerations to support the scaling laws used herein. Key experiments and extensive analytic theory, phenomenological modeling, and computer-based design and systems studies have been carried out. All of the research conducted to date shows that there are no fundamental impediments to successful development of these concepts, and that non-neutronic fusion reactions are readily possible in such devices at relatively small size. Further development is needed to achieve the technologies required for success.

## II. Space Fusion Propulsion Concepts

To be practical, the QED engine must not require massive shielding, and so it therefore must use fuels whose products are only charged particles. The most favorable are those using hydrogen (p) and boron-11 ( ${}^{11}B$ ), and between  ${}^3He$  ions alone.

These reactions proceed according to:<sup>12</sup>



The output kinetic energy of the fusion products can be converted directly into current flow through a series of spherical shell grid structures at specified design potentials. Over 98% of the  ${}^4\text{He}$  products of  $p^{11}\text{B}$  fusion have well-determined energies, with one alpha at 3.82 MeV and two at 2.44 MeV; kinetic-electric conversion efficiency can be made as high as 0.96-0.98 in such a system. For this reaction the maximum emf must be about 1.91 MV (alpha particle charge is  $Z = 2$ ), to hold the energetic  ${}^4\text{He}$  particles from the reaction, and 1.22 MV for the lower energy  ${}^4\text{He}$  fusion product. These voltages can be provided by the external shell and a single collector grid stage within the shell convertor system, so that both particles are collected and removed at their near-zero energy condition after deceleration within the convertor bias field.

The general feasibility of this means of direct conversion has been proven by work at the Lawrence Livermore National Laboratory (LLNL) in earlier (1973-83) research studies.<sup>6,7</sup>

Performance is a function of the system size, electron drive energy, confining  $B$  field (for EXL systems), core convergence in the spherical particle flow, conversion efficiency, and reduction of bremsstrahlung losses by suppression of electron energy at the system center. Detailed computer codes have been developed to solve for ion and electron distributions<sup>13</sup> and power balance in such systems.<sup>14</sup>

Results of one such set of calculations for the  $p^{11}\text{B}$  fuel combination are given in Figures 3a and 3b, which show gross power gain  $G_{gross}$  (electric power generated divided by input electric drive power), and net electric power produced  $P_{net}$  for an EXL system over a range of system sizes and ion accelerating voltages.

This used super-conducting magnets producing 30.8 kG on-axis field at the system surface, an ion core convergence radius ratio of 0.0033, and an overall direct conversion efficiency of 0.94 for the complete system. A fractional central virtual anode height of 0.001 was used, corresponding to a mean energy of 2 keV for core electrons. From the figures, a typical  $p^{11}\text{B}$  fusion-electric source system useful for rocket propulsion would operate at about 250-kV drive voltage, with a radius of 2.5-3.0 m, a gross gain of 32-40, and net electric power of 4500-8000 MWe.

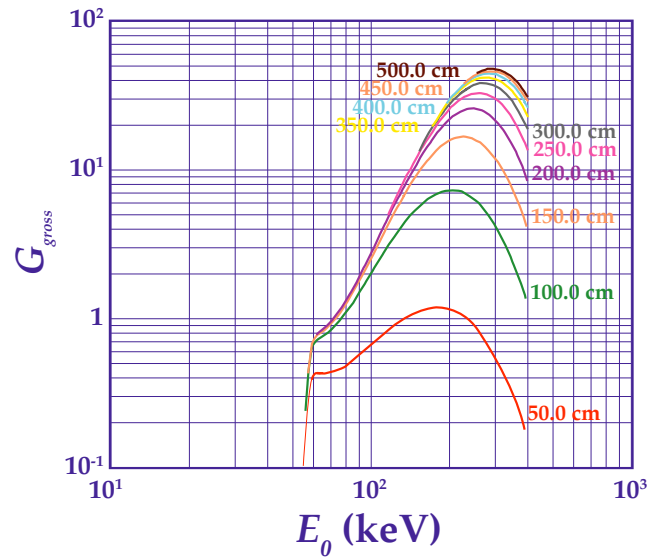


Figure 3a — Gross Electric Gain as a Function of System radius and ion acceleration voltage; EXL system

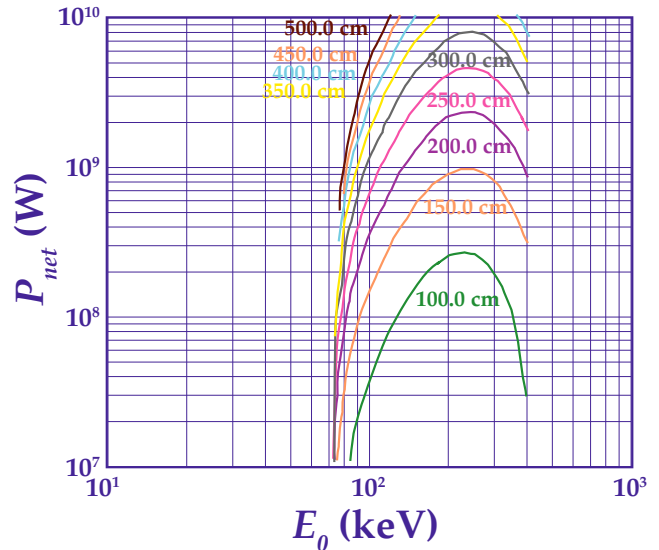


Figure 3b — Net Electric Power as a Function of System radius and ion acceleration voltage; EXL system

The high output voltages from direct conversion are applicable with minimal power conversion to acceleration of rebs for use in high-enthalpy heating of rocket propellants. As suggested previously, the energy of such beams can be deposited essentially completely into rotationally confined and magnetically insulated, high-pressure plasmas to produce very high gas/plasma temperatures. The resulting super-energetic plasma can be exhausted through a magnetically insulated converging-diverging nozzle, to produce thrust at high  $I_{sp}$ . The operating chamber pressure must be optimized for energy deposition profiles to match propellant flow in order to achieve maximum specific impulse from the exit gas at the desired net thrust level of the system. Maximum  $I_{sp}$

will occur at pressures sufficiently high to promote recombination of dissociated and ionized species in the nozzle flow. Figure 4<sup>15</sup> shows such a reb-heated fusion-electric propulsion system.

Unlike an arcjet, here the propellant is heated efficiently (at essentially 100% energy delivery to the propellant) by direct deposition of the reb beam energy into a central core of plasma, surrounded by tangentially injected, radially in-flowing propellant. Thermal radiation from this core is absorbed by the radially inflowing fluid/gas/plasma, which then flows longitudinally along the system axis to the exit nozzle. The keys to efficient heating are nearly complete absorption of thermal radiation in this process, and good coupling of the reb into the central dense plasma. Beam/plasma coupling lengths must be small compared to the reb path through the thruster chamber propellant gas.

Considerable study<sup>16,17</sup> of both high- and low-energy rebs with dense plasmas has shown<sup>18</sup> that unstable beam/plasma interaction lengths for e-folding energy deposition from rebs at the energies of interest here can be made less than 10-30 cm, at (useful) densities the order of  $1E16-1E18/cm^3$ . A thrust chamber length of 1 m would give nearly complete absorption of the e-beam. Current filamentation is easily suppressed by a longitudinal guide field from magnet coils around the system. For example,

a 250-G field will suffice for a reb carrying 1000 MWe at 500 keV and 2000 A, over a beam radius of 4 cm. Modest magnetic fields (ca., 2-8 kG) are also needed to inhibit radial convective heat transfer to the system walls, downstream of the heating region.) Superconducting coils for these guide and insulation fields can be located immediately outside the chamber/nozzle structure and cooled cryogenically, if LH<sub>2</sub> propellant is used, before the propellant is sensibly heated by other regenerative heat loads.

Plasma can be heated by this means, at densities sufficiently high for reasonable thrust chamber dimensions (e.g. 1 m), without excessive or impossible wall thermal loadings, to a maximum temperature on the order of 10 eV (ca., 120,000 K). If used in magnetically insulated nozzles, as shown in analyses by LANL.<sup>19</sup> The specific impulse that can be achieved by nozzle expansion of such plasma depends on the degree to which molecular dissociation and atomic ionization energy can be recovered in the nozzle flow. If no molecular dissociation and atomic ionization energy is recovered with hydrogen propellant at this temperature, then  $I_{sp} = 8000$  s; if they are all recovered, then  $I_{sp} = 12,000$  s. Specific impulse of NH<sub>3</sub> or H<sub>2</sub>O as propellants would be similarly temperature-limited to approximately 3500-5000 s.

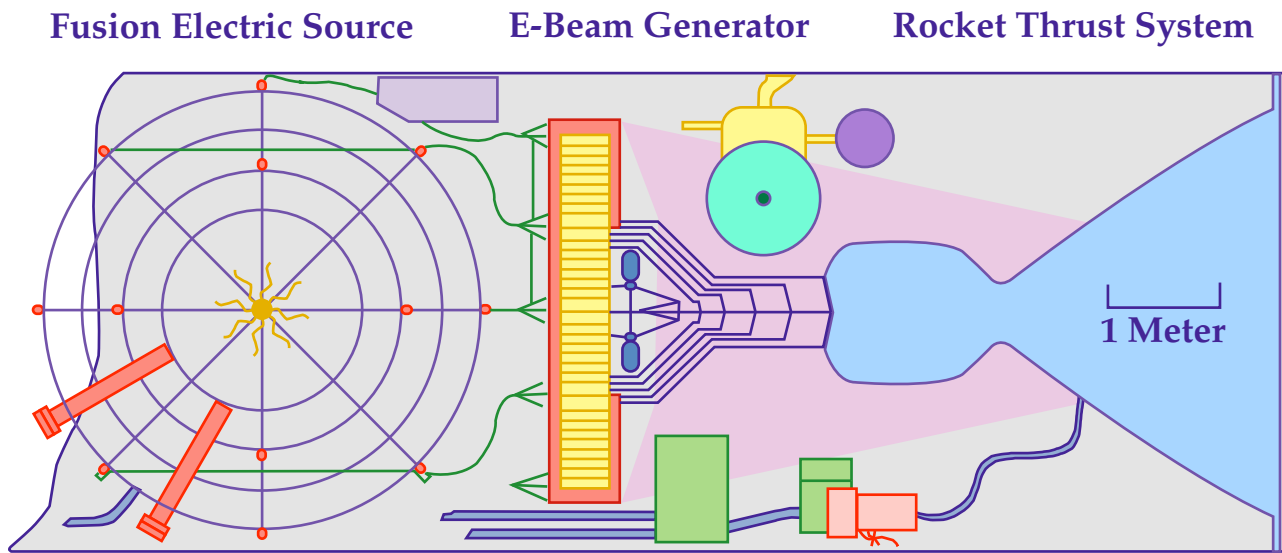


Figure 4 — Schematic outline of ARC/QED engine system

### III. Engine Configurations and Performance

#### A. QED Engine Configurations

Three approaches can be followed for the configuration of QED rocket engine systems.

1. The first of these is an all regeneratively cooled (ARC) engine system, in which the fusion power not deposited into propellant gas by the e-beam is taken up by in-flowing propellant before entering the thrust chamber.
2. Second is a system that utilizes controlled-space-radiation (CSR) cooling to handle some design frac-

tion of the regenerative cooling requirement, so that the in-flowing propellant stream need not accept all of the heat load, and thus can reach higher temperatures, and higher  $I_{sp}$ , or operate at less stringent conditions than for the ARC mode.

3. The third engine type is fundamentally different, in that direct conversion electric power production is used only to drive the source itself, and the fusion product ions are mixed directly with bypass diluent propellant. The energetic propellant mixture from this diluted-fusion-product (DFP) engine system is directed by diversion from a spherical / toroidal magnetic confinement system that has the QED source at its center. By this means the  $I_{sp}$  can be varied from the maximum levels possible in the temperature-limited ARC or CSR systems, to that of the pure fusion products, alone (ca., 1E6 s). The thrust/mass ratio will, of course, vary inversely with increasing  $I_{sp}$ .

The overall performance of these three engine types flows from one to the other, as shown in Figure 5, in comparison with other fusion propulsion concepts.<sup>20</sup> Note that the QED engine systems are all 2-3 orders of magnitude better than any potential competitor. Each of these QED engine systems will be of interest for a differing range of missions, generally those whose characteristic velocity increment is on the order of  $\delta v_c = g_0 I_{sp}$ . Thus, ARC engines fit near-Earth and interplanetary missions best. CSR systems are of the most interest for superfast inner planet interplanetary flights with velocity increment requirements significantly greater than 1E5 m/s, and DFP engines perform best for fast transits to outer planets or in quasi-interstellar missions (e.g., to the Oort Cloud at 500 AU). No further consideration is given here to DFP engine systems.

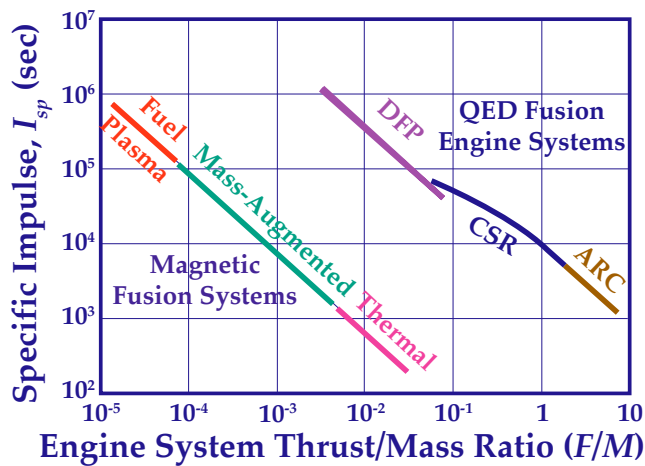


Figure 5 — Comparative performance of ARC/CSR/DFP QED fusion engine systems vs. magnetic fusion propulsion engine concepts,  $I_{sp}$  vs.  $[F]$ .

## B. ARC/QED Engine System

With full regenerative cooling, the maximum enthalpy that can be attained by the propellant before expansion is limited to the ratio of fusion power generated to thermal power losses, multiplied by the maximum limiting enthalpy associated with cooling of the nozzle and chamber walls, and the cooled structures of the fusion power source. Thus, the maximum  $I_{sp}$  that can be attained is given approximately by:

$$I_{spm} = I_{sp0} \sqrt{\frac{P_f}{P_L}}, s \quad (3)$$

Here  $I_{sp0}$  is the specific impulse that could be achieved with propellant gas expansion at the limiting temperature of cooled structures. The engine mass can be related to power, specific impulse, and thrust levels, in terms of its three principal subsystems, as shown in Figure 4. Carrying out this analysis<sup>10</sup> gives a general scaling formula for total system mass as:

$$m_e = P_0 \left( 250 + \frac{400}{I_0^{0.5}} \right) + P_0^{1.67} \left[ \left( \frac{100}{I_0^{1.67}} \right) + 1800 \right] + P_0^{0.5} (K_{iex})(550) + 640, kg \quad (4)$$

where  $P_0 = P_f / 2150$  is the ratio of total fusion power in megawatts, normalized to a point design value of 2150 MW, and  $I_0$  is the ratio of system specific impulse in seconds, normalized to a point design value of 3500 s. The point design mass was  $m_c = 3740$  kg for an IXL system, and 8390 kg for an EXL system.<sup>10</sup>

The factor  $(K_{iex})$  in (4) accounts for the difference in mass between these two types of QED systems. The IXL system has no magnets and  $K_{iex} = 1$ , while the magnetic fields of the EXL system give a coil and subsystem mass that scales as  $K_{iex} = 10$ .

These masses include 540 kg for the thrust system (including nozzle/magnets), 1400 kg (IXL) or 6150 kg (EXL) for the fusion source, and 1800 kg for the electric system (including reb). The source is 2.25 m in outer radius, and it drives the rocket thrust chamber with 4300 A of reb at 500 keV.

This power is dumped into chamber propellant-diluent gas at 10-atmosphere pressure, to give the point design thrust of 11,000 kg. The fusion fuel is p<sup>11</sup>B, driven by an electron injection energy of 250 keV. The direct conversion and associated power loss is 150 MW at the point design power level. Further details of this design have been given elsewhere.<sup>10</sup>

It is of some interest to determine a gross specific mass coefficient ( $a_{fes}$ ) for the engine system, defined as

$$m_{-c} = a_{fes} (1000) (P_f), \text{ kg } (\zeta)$$

where  $a_{fes}$ , is in units of kg/k We, and  $P_f$  is electrical power in MWe. It is obvious from Eqs. (4) and (5) that is not a universal constant for the system, but depends on the values of  $P_o$  and  $I_o$  of interest. Even so, this parameter is useful to compare with alternate electric propulsion systems. For the IXL point design given,  $a_{fes} = 1.74E-3$  kg/k We, thus giving a specific power of 575 kWe/kg; over a thousand times higher specific output than for conventional nuclear (fission) reactor electric space power systems.

Finally, the engine system thrust is related to power and specific impulse by the dimensionless relation:

$$F_o = P_o/I_o \quad (6)$$

where  $F_o = F / 11,000$  is the ratio of system thrust in kg, normalized to a point design value of 11,000 kg (110,000 N). With this the engine system mass can be written in terms of  $I_{sp}$ , and  $F$  [from Eqs. (3) and (5)], thus yielding system thrust-to-mass ratio. Parametric performance of the baseline IXL QED rocket engine systems is as shown in Figures 6 and 7. Note that the thrust-to-mass ratio  $[F]$  ranges from 1.5-6 over the  $I_{sp}$ , range of 1000-6000 s. This performance is two or three orders of magnitude better than that of any other high  $I_{sp}$  engine system for space propulsion.

### C. CSR/QED Engine System

Propellant performance beyond that of regenerative cooling temperature limits can be achieved if a significant fraction of the waste heat is disposed by thermal radiation to space. This, in turn, requires use of (generally massive) space radiators. Such CSR systems will always yield smaller  $[F]$  but higher  $I_{sp}$ , than ARC systems. The total engine system must include the radiator mass  $m_{-rad}$  so that  $m_{-e} = a_{fes} (P_f) + m_{-rad}$ .

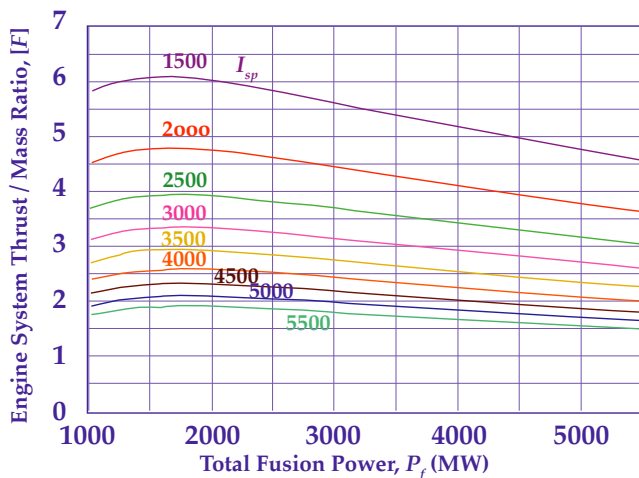


Figure 6 — Thrust-to-mass ratio vs. fusion source power, for various values of specific impulse.

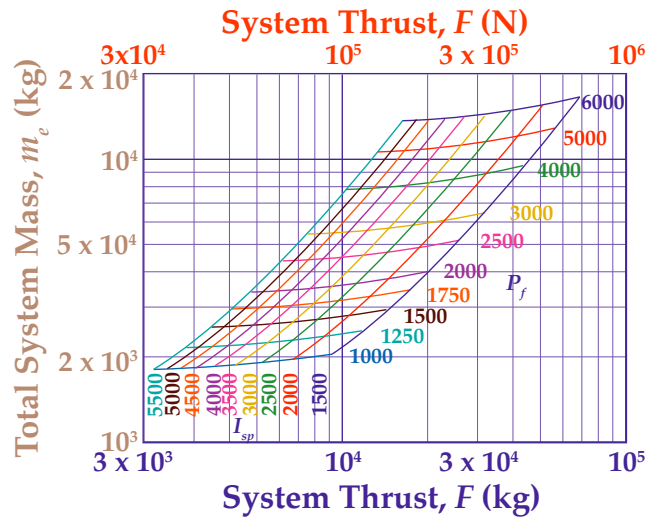


Figure 7 — Parameter map; QED engine system mass and thrust, for varying power and specific impulse.

The radiator mass is:

$$m_{-rad} = a_{rad} (A_{rad}) \quad (7)$$

where the radiating area  $A_{rad}$  is:

$$A_{rad} = \frac{P_{rad}}{\sigma \epsilon T_r^4} \quad (8)$$

$a_{rad}$  is the radiator mass coefficient,  $T$  is radiating temperature, emissivity is  $\epsilon$ , and  $\sigma$  is the Stefan-Boltzmann radiation constant,  $5.67E-12$  W/cm<sup>2</sup>, K<sup>4</sup>.

Now, using the nomenclature of an earlier study,<sup>15</sup> assume a CSR system with a fusion source electric gain of  $G_e = 50$ , so that the recirculating power fraction is simply  $f_{\bar{Q}} = 1/G_e = 0.02$ . As a low-performance example, assume that a large fraction,  $f_L = 0.15$ , of the total fusion power is deposited directly in structure, but that only 0.02 of this (or 0.003 of total power) needs to be regeneratively cooled while the rest ( $f_L = 0.147$ ) is rejected through the waste heat radiator circuit. The remaining 0.85 power fraction is converted directly to electricity at efficiency  $\eta_{-c} = 0.96$ . The unconverted fraction ( $f_r = 0.034$ ) of this power must also be rejected by the radiator.

Thus, a fraction 0.003 of the total fusion power is cooled regeneratively, 0.181 is rejected in a high-temperature waste heat radiator system, and 0.816 is in electrical power that drives the propellant heater or accelerator. The total power fraction going into the propellant stream is 0.819. Then, for a regeneration temperature  $T_{reg} = 1800$  K (2780°F), the upper limit value of  $I_{sp}$  is found to be  $I_{sp} = 11,450$  s.

Finally, assuming that waste heat is radiated only from one side of the surface, with a mass coefficient (based on single-sided area) of  $a_{rad} = 20$  kg/m<sup>2</sup>, and that it operates

with  $\varepsilon = 0.9$  at  $T_r = 2000$  K, the radiator mass can be calculated from Eqs. (7) and (8). above. Taking the CSR engine system specific mass coefficient as  $a_{fs} = 5.0E-3$  kg/kWe (three times larger than cited before), then allows the determination of the complete propulsion system mass.

With these parameters, and accounting for the power regenerated into the propellant, the propulsion system force acceleration can be calculated. Taking a degraded value of 11,000 s for  $I_{sp}$ , the propulsion system thrust-to-mass ratio is found to be  $[F] = 0.103$ . In this example, the radiator mass is found to be about 0.68 of the total engine system mass. This level of performance would allow CSR/QED engine use for high-thrust rocket missions, even in cis-lunar space. For use in deep space missions (beyond the inner solar system), optimum system design would choose still higher  $I_{sp}$  values, with lesser waste heat absorption (i.e. dump all waste heat to space) to minimize radiator mass, while preserving reasonable high thrust capability  $[F]$ .

Finally, the DFP system must use still other means to achieve super-high  $I_{sp}$  to fill its extra-solar mission requirements. This QED engine concept uses the kinetic energy of fusion products directly, varying mean propellant exhaust velocity by mixing these energetic particles with varying amounts of diluent. If the fusion products are used alone, the typical exhaust speed is the order of 1.4E9 cm/s, for a specific impulse of  $I_{sp} = 1.4E6$  s. Dilution by 100:1, for example, reduces this to  $I_{sp} = 140,000$  s. The general range of performance of each QED engine system type is summarized in Table 1.

**Table 1 — Performance range: QED engine systems**

Engine System Type	Isp, Performance Range
ARC	1.5E3 — 0.7 - 1.0E4 s
CSR	0.7E4 — 0.7E5 s
DFP	0.5E5 — 0.7 - 1.0E6 s

## IV. Mission Performance

### A. Single-Stage-to-Orbit Vehicle

Use of an ARC/QED engine system for the SSTO mission has been analyzed and reported elsewhere.<sup>10</sup> This examined a winged single-stage aerospace plane that used conventional turbojet engines for flight propulsion to about  $M = 2-2.5$ , and switched over to QED rocket

propulsion for the remainder of flight to low Earth orbit (LEO). Vehicle flight performance was estimated from the exponential mass-ratio equation, using a net effective specific impulse  $I_s$ , along the flight path, as determined by drag and lift analysis using simplified flat plate models at hypersonic speeds. The flight-speed-averaged value was found to be  $2200 < I_s < 2400$  s; comparable to the performance of conventional subsonic turbojet engines.

The performance analysis showed attainment of LEO at 555 km (300 nautical miles) at 65 minutes after takeoff, with a mass fraction remaining of 0.62 of gross takeoff weight  $m_o$ . This left ample margin for large payload capacity with sturdy structure factors. If vehicle dry weight is  $0.48m_o$ , for example (a reasonable value), the payload capacity would be 14% of  $m_o$ . A 250,000 kg QED vehicle could then deliver 35,000 kg to LEO, and return to a soft horizontal landing at any airfield.

Assuming that the cost of vehicle construction and manufacturing is \$1000/kg, the single-vehicle direct cost would be 120 million dollars. Recovering this over a flight life cycle of 240 flights, (e.g. 24/year for 10 years), the direct capital cost charges amount to only about \$14.29/kg delivered to LEO. Allowing 50% of this (\$7.14/kg) for maintenance costs adds 2.5 million dollars to the cost of each flight. The cost of propellant ( $H_2O$ ,  $NH_3$ ,  $LH_2$ ) at \$1/kg adds an additional \$2.72/kg for a total cost of direct capital investment and operations of \$24.15/kg of payload to LEO.

Furthermore, assume that research and development costs are 10 billion dollars for the complete engine plus vehicle operational system. If these are allocated over 100,000 vehicle flights (e.g., 250 flights/vehicle with 400 vehicles; about 1% of present-day aircraft yearly flight usage), the cost is 100 thousand dollars per vehicle flight. Further assume that profit is allowed at 100% of direct cost of capital and operations. The contribution of each of these cost elements to unit cost is then \$2.86/kg and \$24.15/kg, respectively.

Under these assumptions the total price for payload delivery to LEO is then still only \$51.16/kg. This is to be compared with current launch-to-LEO costs of ca. \$10,000/kg from existing systems, and projected costs of \$300-700/kg for the most realistic models of alternative future Earth-to-space transport systems. Slightly over 47% of this cost is profit at a rate of \$845,250 per flight. This profit generation yields a net rate of return on the 120 million dollars direct capital cost of the vehicle (above) of 16.91%; a respectable margin for a private enterprise system. Conversely, if government owned, with no defined profit generation, costs to LEO would be only \$27.01/kg (\$12.28/lb).

This startling reduction in projected launch costs results from the very large performance of the QED engine; far

beyond that of any other conceptual alternative advanced rocket engine. The cost of a research and development program to test the QED engine principles and to develop a full engine capability is estimated at less than 20% of the vehicle development costs above. And, research and development testing through complete engine concept proof-of-principle could be accomplished for no more than 500-700 million dollars over 7-9 years. If all went well, first flight applications of the QED system could be within 14-16 year of full program initiation. This sort of SSTO would remove the very expensive starting cost (launch-to-LEO) for all manned space exploration missions, greatly reducing overall mission costs.

## B. Interplanetary Missions

The most straightforward system for fast interplanetary flights is the basic ARC engine system, using charged particle power conversion at high efficiency, with only modest power fractions allowed into the regenerative coolant stream. That this is possible is evident from inspection of Figures 3a and 3b. Here, the system gain for  $P_{net} = 6000$  MWe is about 37:1, and for 12,000 MWe it is 46:1 (cf. 50:1 for the CSR example used above).

Since the fast fusion product alpha particles from  $p^{11}B$  fusion appear at relatively precise energies (a result of the unique decay scheme of  $^{12}C^*$ ), it is possible to convert their energy directly to electricity at efficiencies above these  $G_{gr}$  implied values. If 0.98 can be achieved, then less than 0.02 of the gross fusion energy must be taken by ARC cooling streams. Allowing regenerator fluid temperature to be 2000°C permits engine operation with  $I_{sp} \leq 5600$  s. Performance beyond the limit of ARC systems can be obtained only by use of CSR cooling systems, as described above, together with the reduction of regenerative cooling load fractions. Using all of the foregoing analyses for ARC and CSR engine types, mission performance estimates have been made for single-stage vehicle flight between Earth's solar orbit and Mars' solar orbit, to illustrate the enormous performance potential of this generic QED engine concept for inner planet space flight.

Application to outer planet flights requires CSR engines that operate at higher  $I_{sp}$  than can be achieved by ARC systems, if short transit times are desired. But these have a thrust/mass ratio  $[F]$  reduced from that for the ARC engine by the need for the waste heat radiator. The practical limit on  $I_{sp}$  in CSR systems is set by the absolute minimum heat load that must be regeneratively cooled. This is probably at the level of 1 part in 10,000 from marginal but unavoidable X-ray heating of propellant supply piping and superconducting magnet windings. At this level the maximum will be about 50,000-70,000 s, allowing deep space missions with characteris-

tic velocity requirements of 0.5-1E6 m/s. Here, the CSR system thrust/mass ratio will fall in a range of about  $0.08 < [F] < 0.17$ , allowing total vehicle force accelerations of 8-15 milligee (8-15  $mg_0$ )

The variation of  $[F]$  with  $I_{sp}$ , for these QED engines is shown in Figure 5, given previously, as compared with other schemes for fusion propulsion based on conventional magnetic fusion concepts. The general range of each QED engine system type is indicated, as well. Note that the performance of these engines is characteristically two to three orders of magnitude better than the other fusion approaches.

Finally, Figure 8 and Table 2 show space vehicle concepts and flight performance for QED engine-driven vehicles. For comparison, data is also given for a system powered by DD or  $D^3He$  tokamak engines. The scale of these spacecraft is shown in Fig. 8. The top sketch is for the DD tokamak system, that next is for a QED/CSR system with peak  $I_{sp}$  of about 7200 s, below that is an ARC system of higher thrust and shorter burn time, followed by the same system reconfigured to a 6:1 L/D ratio.

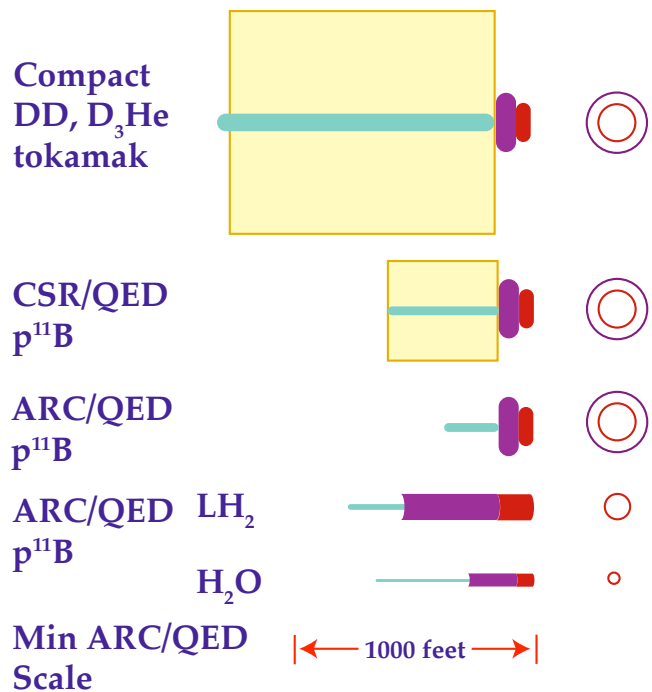


Figure 8 — Earth/Mars vehicle configurations; QED, ARC, and CSR engines vs. compact DD tokamak system

All of these systems have an initial mass in Earth orbit of 10,000 metric tonnes T, and all use  $LH_2$ , as propellant. If the last-referenced system is made to run on  $H_2O$  or  $NH_3$ , as propellant, it will have the same mass distribution, but will be significantly smaller in size. This is shown in the next-to-last figure. Using the same propellants, the very small, last figure is for a minimum ARC system based on the minimum size QED drive unit; it has an in-orbit mass of 500 T.

Table 2 Single-stage Earth-orbit/Mars-orbit flight: QED fusion propulsion engines

Parameter	Compact DD tokamak <sup>15</sup>	CSR/QED	ARC/QED	Minimum ARC/QED	Minimum CSR/QED
$M_o$	10 Mkg	10 Mkg	10 Mkg	500 Kkg	500 Kkg
$M_L$	1.9 Mkg	(a) 1.9 Mkg	1.9 Mkg	72 Kkg	103 Kkg
$M_p$	6.31 Mkg	6.70 Mkg	7.17 Mkg	360 Kkg	335 Kkg
$M_t$	1.00 Mkg	(b) 0.32 Mkg	(c) 0.045 Mkg	20.0 Kkg	16.0 Kkg
$A_{rad}$	3.45 E5 m <sup>2</sup>	6.0 E4 m <sup>2</sup>	0	0	3.0 E3 m <sup>2</sup>
$P_f$	6.63 GW	6.5 GW	13.0 GW	—	—
$P_t$	3.93 GW	6.0 GW	12.0 GW	(d) 6.0 GW	1.0 GW
$I_{spo}$	5235 s	5500 s	5500 s	5500 s	5500 s
$I_{spf}$	7365 s	7800 s	5500 s	5500 s	7800 s
$F_o$	15.0 Kkg	22.5 Kkg	45.0 Kkg	22.5 Kkg	1.88 Kkg
$F_f$	10.7 Kkg	15.9 kkg	45.0 kkg	22.5 kkg	1.33 kkg
$a_o$	1.50 mg <sub>o</sub>	2.250 mg <sub>o</sub>	4.50 mg <sub>o</sub>	45.50 mg <sub>o</sub>	3.76 mg <sub>o</sub>
$a_f$	2.89 mg <sub>o</sub>	4.81 mg <sub>o</sub>	15.9 mg <sub>o</sub>	159.0 mg <sub>o</sub>	8.06 mg <sub>o</sub>
$\delta v_c$	61.2 km/s	73.2 km/s	67.4 km/s	67.4 km/s	71.0 km/s
$t_{b1}$	20.2 days	16.0 days	7.4 days	0.74 days	9.3 days
$\delta S_I$	24.9 Mkm	23.8 Mkm	10.2 Mkm	1.0 Mkm	13.4 Mkm
$t_{c12}$	18.1 days	16.5 days	27.7 days	32.2 days	22.3 days
$\delta S_{I2}$	48.3 Mkm	50.4 Mkm	78.2 Mkm	90.1 Mkm	68.4 Mkm
$t_{b2}$	14.4 days	10.9 days	3.5 days	0.24 days	6.3 days
$\delta S_2$	18.2 Mkm	17.2 Mkm	3.1 Mkm	0.3 Mkm	9.6 Mkm
$t_{total}$	53.3 days	43.4 days	38.6 days	33.2 days	37.9 days
$\delta S_{total}$	91.4 Mkm =	56.8 Mmile	—	—	—

(a)  $M_L = 2.32$  Mkg if  $\delta v_c = 6.12$  km/s,  $t_{total} = 53.3$ d. (b) Two CSR/QED trust systems, one on, one reserve, one radiator system. (c) Two ARC/QED thrust systems; both operating. (d) Both values are thrust power.

The performance of each of these systems is summarized in Table 2, which lists various parameters describing the vehicles and their flight potential. Masses are given for gross, payload, and thrust system (exclusive of propellant). Also tabulated are fusion and thrust power, and initial and final thrust levels and vehicle force accelerations.

All of the flight profiles make use of acceleration and deceleration phases, around a midcourse coast phase. The vehicle characteristic velocity capability (for total propellant expulsion) is listed, and powered and coast times and distances are given. Note that all of the systems offer payloads of 14.4-20.6%, with transit times to Mars' orbit of 33-54 days, over a flight distance of about 90 million km. The mean angle of the flight vector to the tangent to the planetary orbit path is about 40 degrees: this is true "point-and-go" navigation!

All vehicle force accelerations are well above the solar gravity field throughout their flight, thus all flights are high-thrust in character. This eliminates the need for added vehicle characteristic velocity required to lift propellant mass out through the solar field, as is the case for low-thrust systems ( $a < 0.1 mg_0$ ) that must spiral slowly out from the Sun.

The minimum system is of special interest, because of its relatively small in-orbit mass. This vehicle could carry over a 20% payload to Mars' orbit in less than 40 days, with a single-stage flight system. Since it can run on water as propellant, refueling at Mars for the return journey should be feasible. This system is both less massive and smaller in size than the Saturn-5 launch vehicle used in the NASA lunar program.

As a crude estimate of transport costs, consider a system whose manufacturing cost is \$2500/kg. with a lifetime of 100 roundtrips to Mars' orbit, which uses 0.632 of its mass as propellant on each one-way leg of the trip. Assume further that (nonprofit) cost of propellant delivery to launch orbit is the same as estimated previously for the SSTO mission using QED engines, or \$27.01/kg. Allowing 8.0%/annum for cost-of-money, 2% of capital cost for operations and maintenance each flight, and depreciating the vehicle linearly over its 100-trip life, with 3 roundtrips per year, gives a cost of \$209.6/kg payload delivered between Earth and Mars' orbit. Since this is distributed as \$67.0/kg for capital depreciation and O&M, \$59.7/kg for interest, and \$82.9/kg for propellant cost to orbit, further significant reductions will require much higher use rates, longer vehicle life, and reduced cost of propellant supply.

## V. Conclusions

New concepts for electrostatic confinement and control of reactions between fusionable fuels offer the prospect of clean, nonhazardous nuclear fusion propulsion systems of very high performance. These can use either direct-electric heating by relativistic electron beams, or propellant dilution of fusion products. If feasible, QED rocket engine systems may give  $[F] = (4000 - 10,000)/I_{sp}$ , for  $1500 < I_{sp} < 1E6$  s; two to three orders of magnitude higher than from any other conventional nuclear or electric space propulsion system concept.

## Acknowledgments

This work was supported in part by the SDIO/IST Office, and managed by the NASA Lewis Research Center, Cleveland, Ohio, under Contract NAS3-26711. EMC2 also provided internal funding. Other, informal support was given by R. H. W. Waesche at Atlantic Research Corporation, Gainesville, Virginia, who laid out the ARC engine, and by Dana Andrews at Boeing Space and Defense Group, Kent, Washington, who made flight studies of the SSTO vehicle. The author is grateful to these colleagues for their interest and work, and to Harvey Bloomfield of the NASA/LeRC, for his encouragement in this effort.

---

## Revision History

Received April 24, 1993; presented as Paper 93-2006 at the AIAA/SAE/ASME/ASEE 29th Joint Propulsion Conference and Exhibit, Monterey, CA, June 28-30, 1993; revision received April 22, 1994; accepted for publication June 14, 1994. Copyright © 1993 by R.W. Bussard and L.W. Jameson. Published by the American Institute of Aeronautics and Astronautics, Inc., with permission.

Reformatted and color illustrations added May 2007 by Mark Duncan. Minor updates to illustrations and equations December 2008, and references in April 2009.

## References

- <sup>1</sup> Maxwell Hunter; "Solar System Spaceships," *Thrust Into Space*, Holt, Rhinehart and Winston, New York, 1966, Chapter 5.
- <sup>2</sup> Robert W. Bussard and R.D. DeLauer; *Nuclear Rocket Propulsion*, McGraw-Hill, New York, 1958.
- <sup>3</sup> Robert W. Bussard and R.D. DeLauer; *Fundamentals of Nuclear Flight*, McGraw-Hill, New York, 1965.
- <sup>4</sup> Robert W. Bussard; "ASPEN-IL: Two-Staging and Radiation Shielding Effects on ASPEN Vehicle Performance," Los Alamos Scientific Labs. LA-2680, Los Alamos, NM, June 1962, declassified with deletions, Sept. 1967 summarized in "ASPEN: Nuclear Propulsion for Earth-to-Orbit Aerospace Plane Vehicle," *Proceedings of the International Conference on Spaceflight* (Rome, Italy). Pergamon, London, June 1971.
- <sup>5</sup> Robert A. Gross; *Fusion Energy*, Wiley, New York, 1984, Chapters 2 and 3.
- <sup>6</sup> Ralph W. Moir and William L. Barr; "Venetian Blind' Direct Energy Converter for Fusion Reactors," *Nuclear Fusion*, Volume 13, 1973, pp. 35-39.
- <sup>7</sup> William L. Barr and Ralph W. Moir; "Test Results on Plasma Direct Convertors," *Nuclear Technology and Fusion*, Volume 3, 1983, pp. 98-103.
- <sup>8</sup> Robert W. Bussard; "Method and Apparatus for Controlling Charged Particles," U.S. Patent 4,826,626, assigned to Energy/Matter Conversion Corp. (EMC2), Manassas, VA, May 2, 1989.
- <sup>9</sup> Robert W. Bussard; "Method and Apparatus for Creating and Controlling Nuclear Fusion Reactions." U.S. Patent 5,160,695, assigned to QED, Inc., Greenbelt, MD, November 3, 1992.
- <sup>10</sup> Robert W. Bussard; "The QED Engine System: Direct Electric Fusion-Powered Rocket Propulsion Systems," *Proceedings of the Tenth Symposium on Space Nuclear Power and Propulsion*, Univ. of New Mexico, Albuquerque. NM, 1993 (Paper 263).
- <sup>11</sup> H.D. Froning and Robert W. Bussard; "Fusion-Electric Air-Breathing Propulsion for Hypersonic Vehicles," AIAA Paper 93-2611. June 1993.
- <sup>12</sup> D.L. Book; "NRL Plasma Formulary." 1983, revised, Naval Research Lab., Washington, DC, p. 44.
- <sup>13</sup> Katherine E. King and Robert W. Bussard; "EKXL: A Dynamic Poisson-Solver for Spherically-Convergent Inertial Electrostatic Confinement Systems." Annual Meeting of the Plasma Physics Division of the American Physical Society, Paper 2T11, Tampa. FL. November 1991; also *Bulletin of the American Physical Society*, Volume 36, 1991, p. 2319.
- <sup>14</sup> Robert W. Bussard and Lorin W. Jameson; "Power Balance in IEF Systems," *Preliminary Study of Inertial-Electrostatic-Fusion (IEF) for Electric Utility Power Plants*, Electric Power Research Institute, EMC2 Final Report EPRI-TR-103394, Project 8012-16. Section 5.E., Palo Alto, CA, February 1994. pp. 66-77.
- <sup>15</sup> Robert W. Bussard; "Fusion as Electric Propulsion." *Journal of Propulsion and Power*. Vol. 6, No. 5, 1990, pp. 565-573.
- <sup>16</sup> Lester E. Thode and R.N. Sudan, "Plasma Heating by Relativistic Electron Beams. I. Direct Current Interaction." *Physics of Fluids*, Volume 18, No. 11, 1975, pp. 1552-1564.
- <sup>17</sup> Ronald C. Davidson; *Theory of Nonneutral Plasmas*. W. A. Benjamin. Inc., Reading, MA, 1974, Section 2.11, p. 78.
- <sup>18</sup> Lester E. Thode; "Effect of Electron-Ion Collisions on the Nonlinear State of Relativistic Two-Stream Instability," *Physics of Fluids*, Volume 20, No. 12, 1977. pp 2121-2127.
- <sup>19</sup> R.A. Gerwin, *et al.*; "Characterization of Plasma Flow Through Magnetic Nozzles." Air Force Astronautics Lab., AL-TR-89-092. Edwards AFB. CA, February 1990.
- <sup>20</sup> John F. Santarius; "Magnetic Fusion Energy and Space Development." *Proceedings of the 24th Intersociety Energy Conversion Conference*, IEEE, Volume 5, 1989, p. 2525.